Resonant Tunneling Injection Detectors and Imagers

Omer Gokalp Memis[1], John Kohoutek[1], Dibyendu Dey[1], Wei Wu[1] and Hooman Mohseni[1]

[1]*Dept. of Electrical Engineering and Computer Science, Northwestern University, Evanston, IL 60208*

We present a SWIR detector, which combines resonant structures with injection photodetectors. Room temperature dark current of 8nA at 1V and internal quantum efficiency of 72% were measured. 320-by-256 element arrays were fabricated towards focal plane array integration.

Short-wave infrared detectors have been indispensible tools to detect infrared light in many applications, such as homeland security, biomedicine non destructive material evaluation, environmental monitoring, telecommunications and more. Together with the emerging fields such as quantum telecommunications or quantum ghost imaging, these infrared applications demand higher performance detectors. We have previously designed and developed the injection detectors to satisfy these needs, where we have achieved high gain [1], fast response and low jitter [2] and Fano noise suppression [3]. Here, we report on resonant tunneling injection detectors, which combine a resonant geometry with existing injection detector structure. With the resonant tunneling injection detectors, we are also preparing for integration with read-out integrated circuits towards forming a sensitive infrared imager of 320-by-256 pixels.

The resonant tunneling injection detector consists of lattice matched InP/InAlAs/GaAsSb/InAlAs/InGaAs layers grown on InP substrates. The thicknesses of the layers are, in order, 100nm/5nm/30nm/5nm/1000nm. This structure features the characteristic type-II alignment of injection detectors (InP/GaAsSb/InGaAs), but also includes a conduction band quantum well formed by the GaAsSb sandwiched between thin InAlAs layers. The geometry of the device and the band structure along the central axis are shown in Figure 1.

The primary operation principle of the device is the based on the modulation of the voltage of the central GaAsSb layer. In traditional injection detectors, this layer represents a barrier in conduction band and a well in valance band. It is responsible for injecting the electrons from the InP side to the InGaAs side, the rate of this process is controlled by the photo generation of holes in the thick InGaAs layer. In resonant tunneling injection devices, the principle remains similar, but the main mode of transportation through the InAlAs/GaAsSb/InAlAs conduction band barrier becomes tunneling instead of thermionic emission.

The geometry, layer structure, thickness and doping of resonant tunneling injection detector has been developed and optimized using our custom 3-D FEM simulation model [4]. The wafers were grown using metal-organic chemical vapor deposition (MOCVD). They were patterned using photolithography and Cr/Au/Ni metal contacts were deposited using e-beam evaporation and lift-off. The devices were then formed by reactive-ion dry etching (RIE) with methane-hydrogen (CH_4/H_2), in which InAlAs layers also act as etch stop. The sample was coated with a thin layer of SiO_2 for passivation using plasma-enhanced chemical vapor deposition (PECVD). Finally, the individual devices were made accessible by opening up the SiO_2 layer over the metal contacts.

The devices were tested for dark current and photo-response using a computerized setup. For optical measurements, the devices were illuminated with a CW laser at 1500 nm, which was calibrated using a commercial PIN detector in the same setup. The devices had a injector radius of 5 μm, and showed dark current values of 2.3 nA at 200 mV bias, 4.5 nA at 500mV and 8.4 nA at 1V (Figure 2). Using photoresponse, the internal quantum efficiency of the resonant tunneling injector detectors were measured, which is around 72% at 1 V and exceeded 90% at 2.5 V bias (Figure 3). The spatial response of the devices is also tested, and the active diameter of the devices was recorded as be 30 μm.

In contrast to previous injection detectors, the resonant tunneling injection detectors also exhibited photovoltaic response. Around 0 V, the devices had extremely small dark current (~10pA) with an internal quantum efficiency of 35~40%.

Once the devices were tested for dark/photo-response and characterized, additional processing was performed on the samples towards flip-chip integration. First, a connection from the top surface to the back ground contact needed to be established. To achieve this, SiO_2 passivation on the sample was removed over parts of the sample and the opening was isotropically etched using hydrobromic acid. Then a metal lift-off was performed over the sample to short large mesas around the focal plane array to the ground connection of the sample. After the ground connection, under bump metallization and seed layers are deposited by e-beam evaporation. The devices are

978-1-4244-3681-1/09/$25.00 ©2009 IEEE

coated and patterned with 10 µm thick photoresist, using which indium was electroplated selectively. Finally the seed layer was etched, and the indium bumps were reflown, which made the focal plane arrays ready for integration.

We have processed dies of 320 by 256 pixels focal plane arrays of resonant tunneling injection detectors. A suitable read-out integrated circuit (ROIC - ISC9705 from Indigo) was chosen for compatibility with pixel sizes, and current levels, and had undergone a similar process to prepare for flip chip bonding. The next step for us is to integrate the ROIC with the detector array and get image/videos from the focal plane array. Our initial test and trials on the integration have been successful.

We have designed a new short wave infrared detector by combining resonant structures with our injection detector technology. The device is built around a unique resonant type-II band alignment, and a compatible process flow was designed. Fabricated devices show low dark current values (2-8 nA) at bias voltages of 0.2~1 V. The internal quantum efficiency was measured as a function of voltage, and the spatially active diameter of 10 µm injector devices was 30 µm. A second process flow was created for 320 by 256 element arrays of the resonant tunneling injection detectors, which were fabricated towards focal plane array integration.

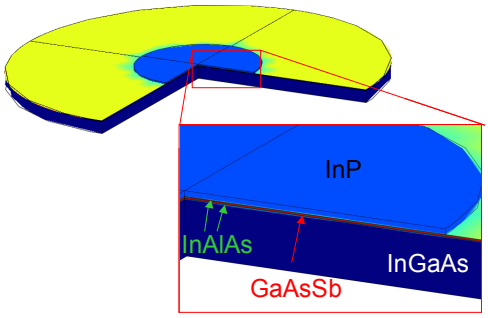

Figure 1 - The geometry and cross section of the device. The inset shows individual layers.

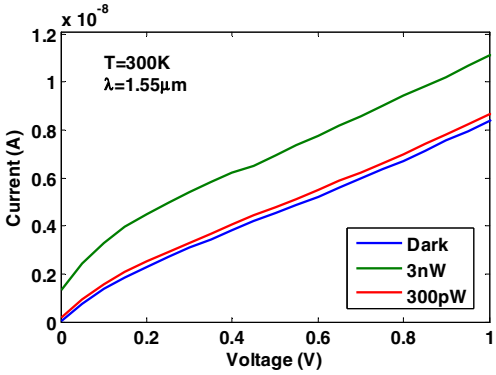

Figure 2 – The dark current and photo-current versus voltage plots of the devices with 10 µm diameter injector at room temperature.

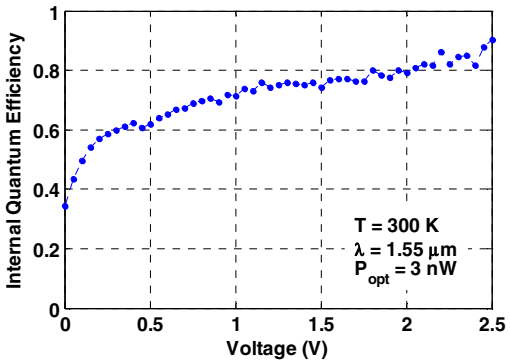

Figure 3 – The internal quantum efficiency of the device at different voltages.

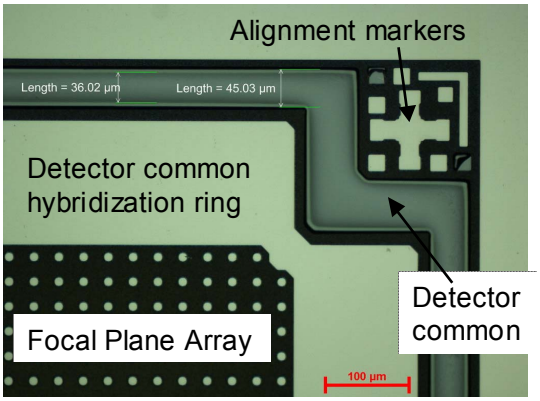

Figure 4 – A microscope image of the detector array being prepared from focal plane array integration.

References:
[1] O.G. Memis, A. Katsnelson, S. C. Kong, H. Mohseni, M. Yan, S. Zhang, T. Hossain, N. Jin, and I. Adesida, "A Photon Detector with Very High Gain at Low Bias and at Room Temperature", *Applied Physics Letters,* 91, pp. 171112 (2007).
[2] O.G. Memis, A. Katsnelson, H. Mohseni, M. Yan, S. Zhang, T. Hossain, N. Jin, and I. Adesida, "On the Source of Jitter in a Room-Temperature Nanoinjection Photon Detector at 1.55 µm", *IEEE Electron Device Letters*, 29(8), pp. 867, (2008).
[3] O.G. Memis, A. Katsnelson, S. C. Kong, H. Mohseni, M. Yan, S. Zhang, T. Hossain, N. Jin, and I. Adesida, "Sub-Poissonian Shot Noise of a High Internal Gain Injection Photon Detector", *Optics Express*, 16(17), pp. 12701 (2008).
[4] O.G. Memis, W. Wu, D. Dey, A. Katsnelson and H. Mohseni, "Detailed Numerical Modeling of a Novel Infrared Single Photon Detector for λ > 1µm", *7th International Conference on Numerical Simulation of Optoelectronic Devices*, pp. 63-64 (2007).